stable conformation, TGGT, is not the only one that is available to reduce density from the amorphous material. We conclude that since, on annealing, the crystal structure of PPT assumes a nonplanar helix-like structure, the difference in conformation of the methylene groups leads to little difference in the effectiveness of close packing of the chains. During the conformational reorganization of the initial state, other less stable conformations such as GTTG also appear to help the chains pack, resulting in an increase in density. The density of crystalline PET, 1.46 g/mL, is significantly higher than that of PPT, 1.39 g/mL.

Acknowledgment. This work was supported by the Polymers Program of the National Science Foundation, Grant DMR-8304220. We thank Dr. R. Kitamaru for the sample of PPT.

Registry No. PPT (SRU), 9022-20-2; PPT (copolymer), 25610-17-7.

References and Notes

(1) Dandurand, S. P.; Perez, S.; Revol, J. R.; Brisse, F. *Polymer* **1979**, *20*, 419.
(2) Desborough, I. J.; Hall, I. H.; Neisser, J. Z. *Polymer* **1979**, *20*, 545.
(3) Smith, J.; Kibler, C.; Sublett, B. *J. Polym. Sci, Part A-1* **1966**, *4*, 1851.
(4) Horii, F.; Hirai, A.; Murayama, K.; Suzuki, T.; Kitamaru, R. *Macromolecules* **1983**, *16*, 273.
(5) Ward, I. M.; Wilding, M. A. *Polymer* **1977**, *18*, 327.
(6) Ward, I. M.; Wilding, M. A.; Brody, H. *J. Polym. Sci., Polym. Phys. Ed.* **1976**, *14*, 263.
(7) Bulkin, B. J.; Lewin, M.; McKelvy, M. L. *Spectrochim. Acta, Part A* **1985**, *41A*, 251.
(8) Bulkin, B. J.; Lewin, M.; DeBlase, F. J. *Macromolecules* **1985**, *18*, 2587.
(9) Kim, J. S.; Lewin, M.; Bulkin, B. J. *J. Polym. Sci., Polym. Phys. Ed.*, in press.
(10) DeBlase, F. J.; McKelvey, M. L.; Lewin, M.; Bulkin, B. J. *J. Polym. Sci., Polym. Lett. Ed.* **1985**, *23*, 109.
(11) Schultz, J. *Polymer Materials Science*; Prentice-Hall: Englewood Cliffs, NJ, 1974.
(12) See, for example: Mandelkern, L. *Crystallization of Polymers*, McGraw-Hill: New York, 1964.

Kinetic Model for Tensile Deformation of Polymers. 1. Effect of Molecular Weight

Yves Termonia* and Paul Smith†

Central Research and Development Department, Experimental Station, E. I. du Pont de Nemours and Company, Inc., Wilmington, Delaware 19898. *Received July 28, 1986*

ABSTRACT: A new comprehensive kinetic model for the tensile deformation of solid, flexible polymers is presented. The model, which is based on the Eyring chemical activation rate theory, explicity takes into account the role of the weak attractive forces between chains as well as chain slippage through entanglements. Stress–strain curves calculated for melt-crystallized polyethylene are in quantitative agreement with experiment.

Deformation of solid polymers is a very complex subject of great technological and theoretical interest. A number of models have been proposed to describe the various phenomena that may occur during deformation, such as brittle fracture, yielding, strain hardening, etc.[1-5] Most models are, however, only phenomenological or semiquantitative, static representations, which are incapable of providing a unified description of the various morphological changes that may occur depending on the dynamics and on the structure at the molecular level. Here we present a new comprehensive kinetic model for tensile deformation of solid, flexible polymers. The model, which is based on the Eyring activation rate theory,[6] explicitly takes into account the role of the weak attractive forces between chains as well as chain slippage through entanglements. Stress–strain curves calculated for melt-crystallized polyethylene are in quantitative agreement with experiment. The model also reveals the wide variety of morphological changes that may occur during tensile deformation of polymers.

The undeformed (isotropic) polymer solid is represented by a dense network of coiled, entangled macromolecules (Figure 1). Note that no details of the crystallites in the solid are specified.[7] We start with the regular array of entanglements depicted in Figure 1b. The molecular weight between entanglements is independent of the chain length;[8] i.e., the number of entanglements per macromolecule increases linearly with its length. The network is elongated at constant rate $\dot{\epsilon}$ and at temperature T along the y axis. This causes straining of the weak van der Waals (vdW) bonds, which break, according to the kinetic theory of fracture,[9] at a rate

$$\upsilon = \tau \exp[-(U - \beta\sigma)/kT] \quad (1)$$

In eq 1, τ is the thermal vibration frequency, and U and β are respectively the activation energy and volume. σ is the local stress: $\sigma = K\epsilon$, where ϵ is the local strain and K is the elastic constant of the bond. The breaking of the vdW bonds along a chain strand between two entanglements leads to a transfer of the external load to the now effectively isolated chain strand. As the load increases upon further deformation, slippage of that chain through entanglements sets in. It is assumed[4-6] that this occurs at a rate that has the same functional form as that of the vdW bond breakings (eq 1), but with different values for the activation energy U and the activation volume β. Now, σ represents the difference in stress in the two strands of a chain separated by an entanglement. In order to estimate that stress, we turn to the classical theory of rubber elasticity.[4] According to this theory, the stress on a chain strand having a vector length r is

$$\sigma = \alpha\, kT\mathcal{L}^{-1}(r/nl) \quad (2)$$

where n is the number of statistical chain segments and

† Present address: Materials Program and Department of Chemical and Nuclear Engineering, University of California, Santa Barbara, CA 93106.

0024-9297/87/2220-0835$01.50/0

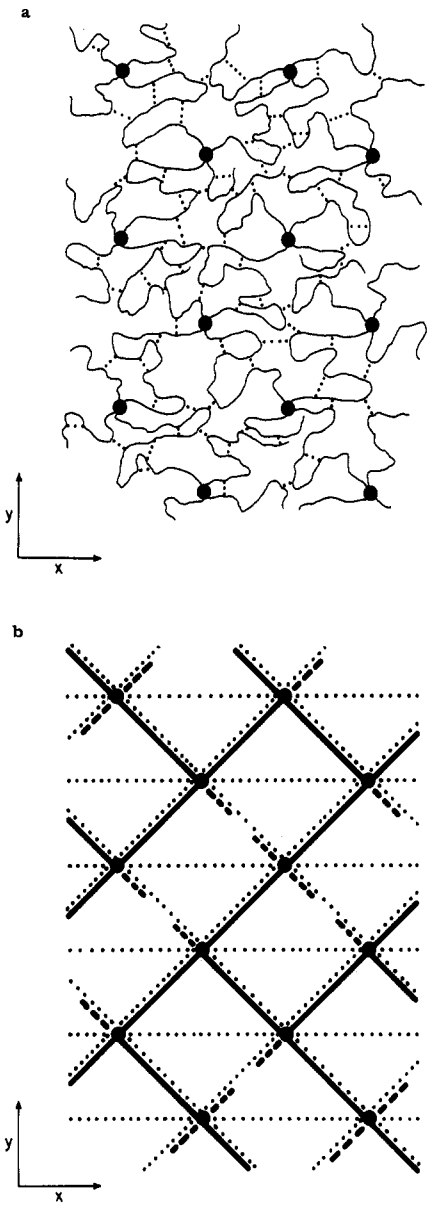

Figure 1. (a) Schematic representation of the undeformed polymer solid. Prior to deformation, the chain segments between entanglements are tied together through numerous weak inter- and intramolecular bonds, e.g., van der Waals forces (dotted lines). The latter provide the initial stiffness to the material. Since the coordination number of an entanglement is only 4, the three-dimensional network, for convenience, has been given a planar (x–y) conformation. (b) A more schematic representation of the network, in which the details of the chain configurations are omitted altogether. The individual van der Waals bonds are replaced by "overall" bonds (dotted lines) joining each entanglement point to its neighbors. The heavy solid lines denote chain vectors between entanglements; chain ends are indicated by dashed lines. The chain vectors in an actual, undeformed specimen are randomly oriented in three-dimensional space; i.e., $\langle \cos^2 \theta \rangle = {}^1/_3$, where θ is the vector's angle with the draw axis. In our simplified, regular two-dimensional representation (b), we thus take the same initial value $\theta = 54.7°$ for all vector orientations along the y axis.

l is their length. $\mathcal{L}^{-1}$ is the inverse Langevin function and α is a proportionality constant that depends on the number N of chain strands per unit volume. Following Treloar[10]

$$\alpha = (N/3)n^{1/2} \tag{3}$$

In accordance with reported experimental results for viscous flow of paraffins,[11] we assume that the average length of a hydrocarbon chain capable of a coordinated movement at a rate given by eq 1 is approximately 25 carbon atoms.

The kinetic model described above was simulated on an array of 7200 entanglement points. The simulation of the vdW bond breakings is performed with the help of a Monte Carlo lottery that breaks a bond i according to the probability

$$P_i = \upsilon_i/\upsilon_{max} \tag{4}$$

Here, υ_{max} is the rate of breakage of the most strained bond in the array. After each visit of a bond, the time t is incremented by $1/[\upsilon_{max}n(t)]$, where $n(t)$ is the total number of intact bonds at time t. For reasons of simplicity, broken vdW bonds are assumed not to re-form during the deformation process.

The simulation of chain slippage through entanglements is executed by using a similar technique; $n(t)$ now denotes the total number of entanglements left at time t. The slippage process leads to a change in the number of statistical chain units between entanglements and, occasionally, to chain disentanglement. If the rate of slippage is too low, however, maximum elongation of the chain strands between entanglements can be reached and chain fracture occurs.

After a very small time interval δt has elapsed, the bond-breaking and chain slippage/fracture processes are stopped and the network is strained along the y axis by a small, constant amount determined by the strain rate $\dot{\epsilon}$. The network is then relaxed to its minimum-energy configuration, using a series of fast computer algorithms described in ref 12. This leads to displacement of the entanglement points along the x and y axes. In order to save computer time, only displacements along the draw axis are explicitly calculated. Distances in the transverse x direction are assumed to be contracted homogeneously by a factor $\lambda^{-1/2}$, where λ is the draw ratio ($\epsilon + 1$) along the y axis. After these relaxation steps, which are the most time-consuming processes in the computer simulation, the axial nominal stress at one end of the network is calculated. The Monte Carlo process of bond breakings and slippage is then restarted for another time interval δt. And so on and so forth until the sample breaks.

The presented model will now be applied to study the effect of the molecular weight on the tensile deformation of melt-crystallized polyethylene. This problem was selected because there exists a wealth of experimental data against which the theoretical results can be verified.

The molecular weight of a statistical chain segment is about 140, and $l \simeq 10$ Å.[13] The atomic vibration frequency τ was taken to be 10^{12}/s, and we chose a strain rate of $\dot{\epsilon}$ = 5/min. A deformation temperature of 75 °C was selected, rather than, e.g., room temperature, to relate to the important drawing processes that are employed to produce high-modulus polymer.[14,15] Values for the other parameters are as follows.

udW Bond Breakage. The elastic modulus K of the vdW bonds was taken to be 4 MPa.[16] We chose U = 30 kcal/mol, which is the activation energy necessary to break 20–30 vdW bonds.[17] Concomitantly, we took $\beta = (26 \text{ Å})^3$.

Chain Slippage. The molecular weight between entanglements in an undiluted polyethylene melt is about 1900[18] and is assumed to be preserved in solids derived therefrom.[19] This corresponds to $n \sim 14$ statistical segments. The density of solid linear polyethylene is about 0.96 g/cm^3, which leads to $N = 3.04 \times 10^{26}$/m^3 chain strands between entanglements. We chose U = 20 kcal/mol with $\beta = (7 \text{ Å})^3$. The latter value is of the order of magnitude of the volume of a statistical chain segment and is consistent with the commonly accepted idea (ref 20

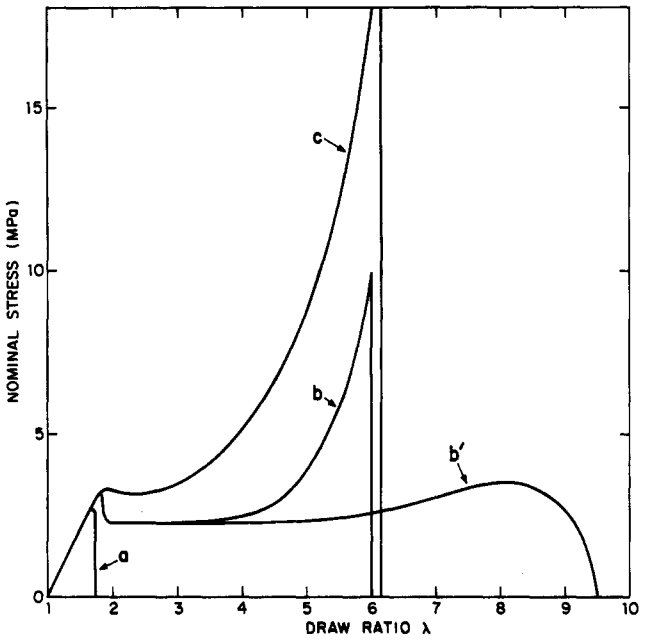

Figure 2. (a–c) Nominal stress–strain curves, calculated under the assumption of no chain slippage, for three monodisperse polyethylenes of M = 1900 (a), M = 9500 (b), and M = 250 000 (c). These results show that the three samples are predicted to exhibit an identical behavior at elongations up to ~75% (i.e., a draw ratio of 1.75), which is indicative of homogeneous loading of the vdW bonds. At draw ratios exceeding ~1.75 the vdW bonds start breaking, and the three specimens display a markedly different behavior. The lowest molecular weight sample (a) shows a stress-strain curve typical of brittle failure. The somewhat higher molecular weight material (b) displays a distinct, so-called yield point (the first maximum in the stress–strain curve), a drawing region, and, finally, strain hardening. The stress–strain curve of the highest molecular weight specimen (c) hardly displays a distinct yield point, and strain hardening sets in immediately after the linear portion of the stress–strain curve. Also, much higher stress levels are reached in the latter case. Curve b′ for M = 9500 is calculated including chain slippage. This phenomenon causes a large increase in the drawability of the material and a smoothening of the strain-hardening effect. The stress–strain curves calculated for the low (M = 1900) and high (M = 250 000) molecular weight specimens are nearly identical in the presence or absence of chain slippage.

and note below eq 4) that slippage involves the coordinated movement of 1–2 statistical segments at most. Our value for β thus appears to be more realistic than that required in previous attempts to fit Eyring's activation theory to experimental data on flow in polymers.[21]

Figure 2 shows a series of stress–strain curves that were calculated with the model for melt-crystallized polyethylenes of different monodisperse molecular weights (M = 1900, 9500, and 250 000). In the first series of simulations (curves a, b, and c) no chain slippage was assumed to occur during deformation. Careful examination of the results of the simulations leads to the following insight and rationale for the marked differences in the stress–strain behavior of the three samples. Let us first consider curves a and b, which correspond to the low molecular weight specimens. In these samples the majority of the vdW bonds exist between strands of different chains. As a result, when one such bond along the y axis breaks, the load it carried has to be transferred to the neighboring vdW bonds. These neighboring bonds become overstressed and easily break in turn. Since the concentration of chain ends is high, there again is a high probability that this vdW bond breaking will lead to a load transfer not to a chain strand but, rather, to the next-neighbor vdW bonds. The latter then break in turn. And so on and so forth. In this way, a crack propagates transversely, meeting occasionally a few intact chain strands, which are then deformed due to the high local stress they have to sustain. As the overall strain is increased, deformation continues entirely within the crack region, because it has a much lower stiffness than the surrounding material due to the small number of chain strands extending across the crack.

If that number of strands is sufficiently high, i.e., at not too low molecular weight (curve b), the local stress in these chains increases (eq 3) upon further deformation to reach the yield stress. This is attained at a local draw ratio of ~4. At this point vdW bonds break in the weakened adjacent undeformed region, leading to the incorporation of more chain strands into the deformed region, or "neck". The neck then propagates along the whole length of the sample. This propagation stage is found to extend from an overall λ = 1.75 to ~4, and it is characterized by a constant value of the (nominal) stress (see curve b). At draw ratios exceeding 4, the deformation proceeds homogeneously through further stretching of the polymer chains. This causes the so-called strain hardening that is observed experimentally.[1-5] It is reproduced in the model without the need to invoke strain-induced crystallization at high degrees of chain extension. The network finally fails at $\lambda_{max} = 14^{1/2}3^{1/2}$, when the chain strands between entanglements have reached full extension (the factor $3^{1/2}$ results from network considerations; cf. ref 22).

For very low molecular weight specimens (curve a, Figure 2) the number of chains that extend across the initial (transverse) crack is too small to carry the external load. The chains rapidly reach full extension and break.

At much higher molecular weights (curve c) the concentration of chain ends is low. As a result, any vdW bond breaking, occurring at $\lambda > 1.75$, leads to load transfer to a chain strand and no local buildup of stress is observed. The network, therefore, deforms homogeneously at all λ and the strain-hardening effect is observed almost immediately past the yield point.

Next, we incorporate the effect of slippage of chains through entanglements on the stress–strain behavior (see Figure 2). Curve b′, calculated for M = 9500, reveals that including chain slippage causes a large increase in the drawability of the material and a smoothening of the strain-hardening effect (cf. curve b). Further investigation shows that chain slippage increases the average molecular weight between entanglements by a factor of ~2. This leads to an estimated maximum draw ratio of $\lambda_{max} = (2 \times 14)^{1/2}3^{1/2} = 9.2$, in excellent agreement with the observed value (Figure 2, curve b′). The stress–strain curves calculated for the low (M = 1900) and high (M = 250 000) molecular weight specimens were found to be nearly identical in the presence of chain slippage or in the absence of it.

Figure 3 displays a schematic illustration of the "morphologies" obtained with the model for the various molecular weights studied. At M = 1900, brittle fracture is observed (Figure 3a); at M = 9500, a well-defined neck appears, which then propagates along the sample (Figure 3b); and at M = 250 000 (Figure 3d), the deformation appears to be homogeneous throughout the entire simulation. Figure 3c depicts the deformed specimen of an intermediate molecular weight M = 20 000, for which multiple necking is observed.

These theoretical results are in outstanding agreement with experimental observations.[1-5] An exhaustive comparison with experimental results as well as detailed studies of the effects of temperature, strain rate, molecular weight distribution, and entanglement spacing on the

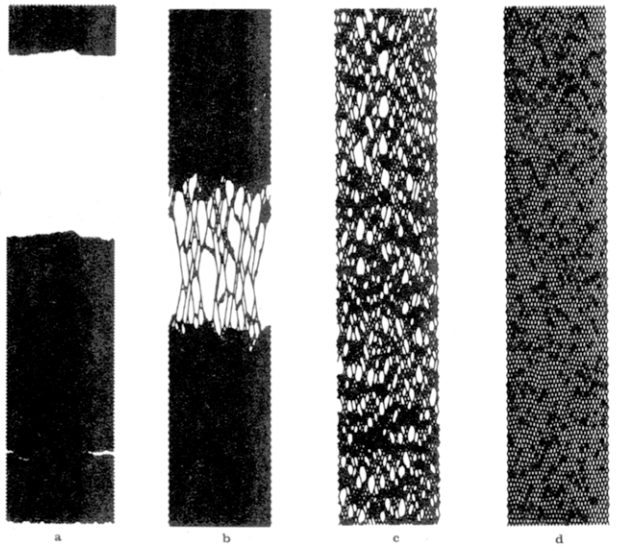

Figure 3. Typical "morphologies" obtained with the model for polyethylene of different monodisperse molecular weights: (a) $M = 1900$ $\lambda = 1.75$; (b) $M = 9500$, $\lambda = 2$; (c) $M = 20000$, $\lambda = 2.5$; (d) $M = 250000$, $\lambda = 3$.

deformation process will be presented elsewhere.

Registry No. Polyethylene, 9002-88-4.

References and Notes

(1) Ward, I. M. *Mechanical Properties of Solid Polymers*, 2nd ed.; Wiley: New York, 1983.
(2) Kinloch, A. J.; Young, R. J. *Fracture Behavior of Polymers*; Applied Science: London, 1983.
(3) Ferry, J. D. *Viscoelastic Properties of Polymers*, 3rd ed.; Wiley: New York, 1980.
(4) Treloar, L. R. G. *The Physics of Rubber Elasticity*, 2nd ed.; Clarendon: Oxford, 1958.
(5) Kausch, H. H. *Polymer Fracture*; Springer Verlag: Berlin, 1978.
(6) Glasstone, S.; Laidler, K. J.; Eyring, H. *The Theory of Rate Processes*; McGraw-Hill: New York, 1941. Ree, T.; Eyring, H. In *Rheology*; Eirich, F. R., Ed.; Academic: New York, 1958, Vol. 2, p 83.
(7) This simplification appears justified for deformation at elevated temperatures of semicrystalline solids of weakly bonded macromolecules (see, e.g.: Meinel, G.; Peterlin, A. *J. Polym. Sci.* **1971**, *9*, 67 and ref 15), to which the model currently is restricted. Under such experimental conditions the role of the crystals is limited to providing a very viscous medium that prevents recoiling of deformed macromolecules.
(8) Graessley, W. W. *Adv. Polym. Sci.* **1974**, *16*.
(9) E.g., overview in ref 5, p 53.
(10) Reference 4, p 107.
(11) Kauzmann, H.; Eyring, H. *J. Am. Chem. Soc.* **1940**, *62*, 3113.
(12) Termonia, Y.; Meakin, P.; Smith, P. *Macromolecules* **1985**, *18*, 2246; **1986**, *19*, 154.
(13) Flory, P. J. *Statistical Mechanics of Chain Molecules*; Interscience: New York, 1969; p 12.
(14) See, e.g., Chapters, 1, 2, 10, and 11 by respectively G. Capaccio et al., A. E. Zachariades et al., A. J. Pennings et al., and A. Peterlin and A. Keller In *Ultra-High Modulus Polymers*; Ciferri, A., Ward, I. M., Eds.; Applied Science: London, 1979.
(15) Smith, P.; Lemstra, P. J.; Booij, H. C. *J. Polym. Sci., Polym. Phys. Ed.* **1981**, *19*, 877.
(16) Consistent with our ignoring the details of the crystals, we take the value 4 MPa for the elastic constant of van der Waals bonds. This value was obtained (Smith, P., unpublished) by extrapolating the initial modulus of molten ultrahigh molecular weight polyethylene to the "test" temperature of 75 °C. As a result of this simlification, the calculated initial moduli in Figure 2 are below those found experimentally.
(17) Indeed, we recall that our model is expressed in terms of "overall" bonds which represent all the van der Waals bonds existing along a chain strand between two entanglements (see Figure 1b).
(18) Porter, R. S.; Johnson, J. F. *Chem. Rev.* **1966**, *66*, 1.
(19) Flory, P. J.; Yoon, D. Y. *Nature (London)* **1978**, *272*, 226.
(20) Reference 4, pp 298–299.
(21) Haward, R. N.; Thackray, G. *Proc. R. Soc. London Ser. A* **1968**, *A302*, 453.
(22) Kramer, E. J. *Adv. Polym. Sci.* **1983**, *52/53*, 33.